

# Gyrokinetic simulations of multi-scale turbulence on the supercomputer Fugaku

Shinya Maeyama

Nagoya University

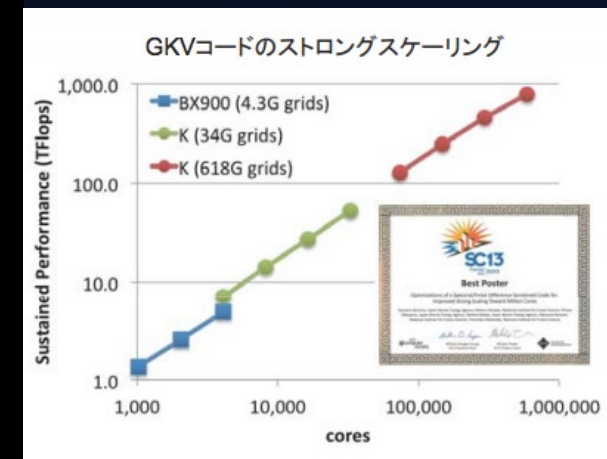
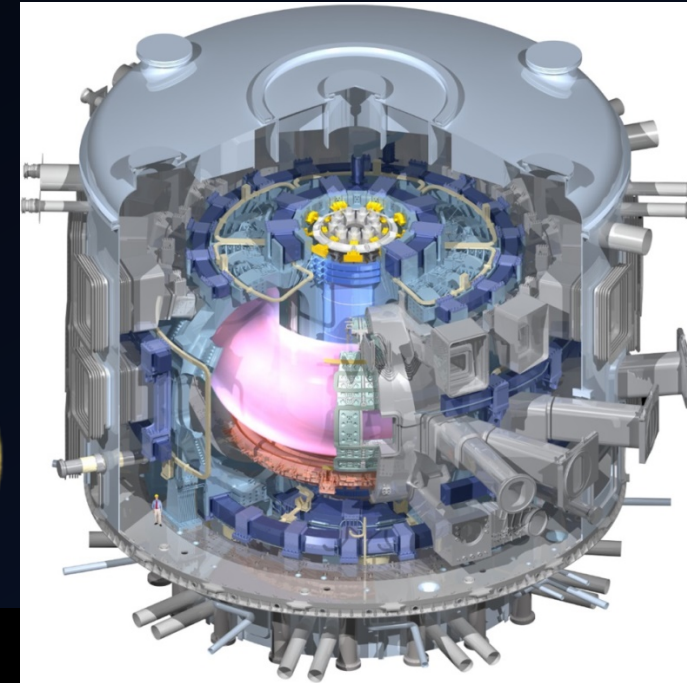
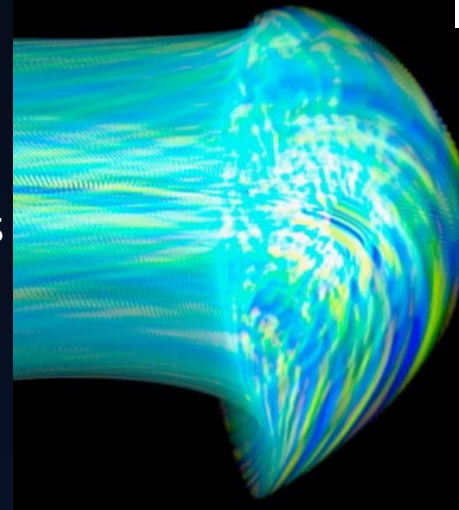
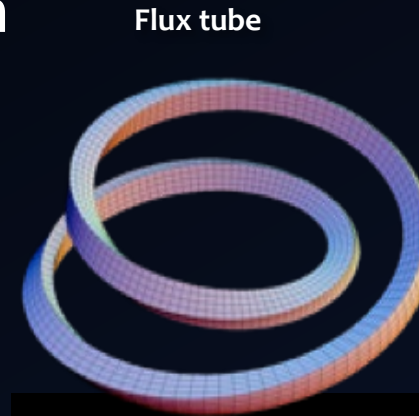
IFERC Workshop on GPU Programming 2021, virtual, 14 June 2021

# Outline

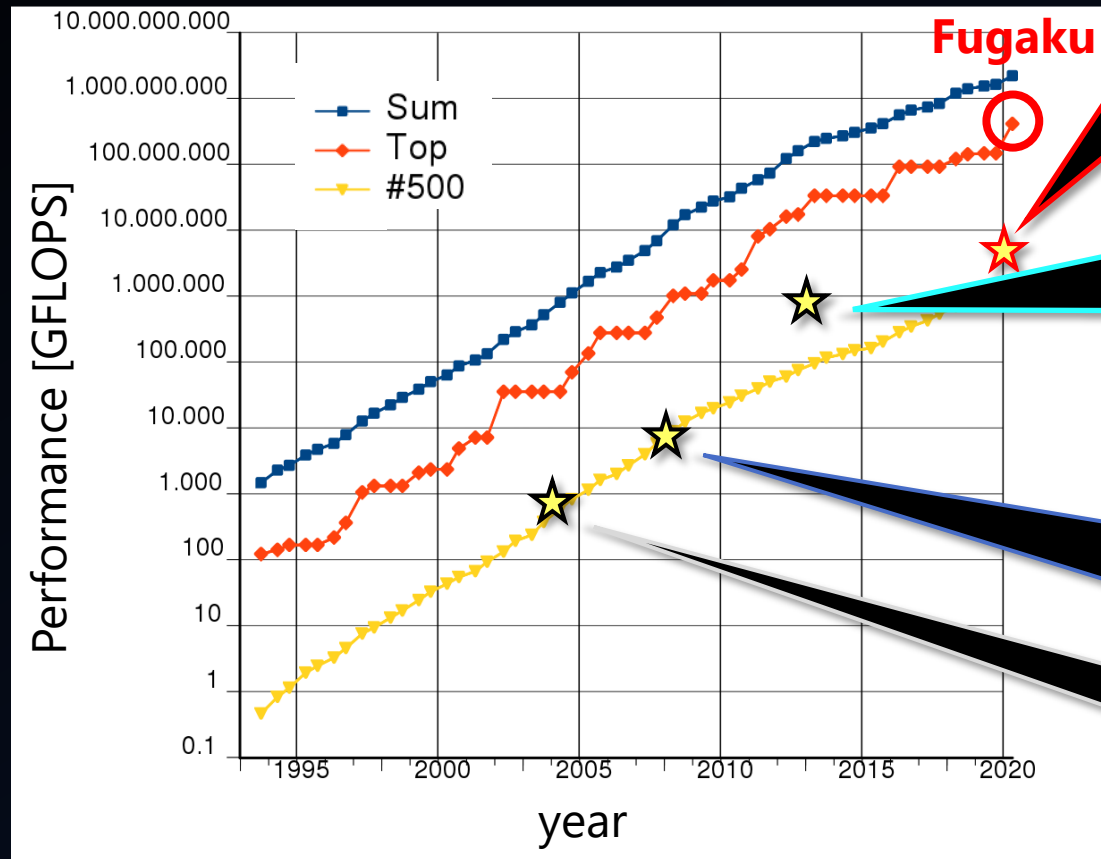
- Optimization of GKV code on the supercomputer Fugaku - 10 min
- Multi-scale turbulence simulations toward burning plasma - 10 min

# GyroKinetic Vlasov code GKV

- Plasma turbulence simulation based on delta-f gyrokinetic model
- 5D Eulerian solver
  - Fourier spectral method( $x, y$ ) + Finite difference( $z, v_{\parallel}, \mu$ )
  - Explicit + implicit (collision) time integration
  - MPI/OpenMP hybrid parallelization
- High resolutions in local flux tube geometry
  - Multi-scale simulation from ion to electron scales
  - Multi-species collision
- Free download
  - <https://p.phys.nagoya-u.ac.jp/gkv/>
  - <https://github.com/GKV-developers/gkvp>

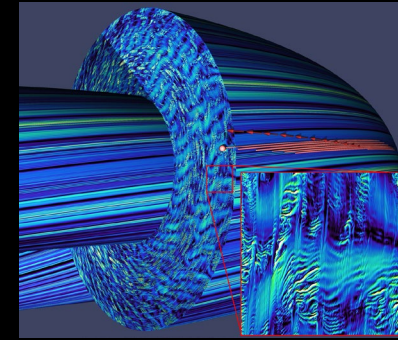


# GKV as an HPC application



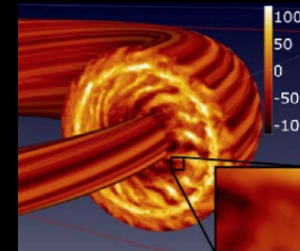
Physics model of GKV is extended along with HPC.

Multi-scale turbulence simulations for burning plasma (e, D, T, He)

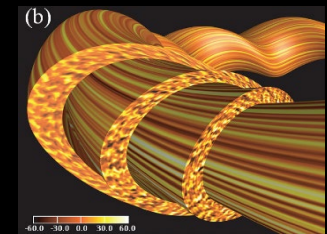


NOTE: Performance of GKV on Fugaku 12288 nodes (March 2021)

Multi-scale turbulence simulations for hydrogen-electron plasma  
cf. Maeyama, et al., Phys. Rev. Lett. (2015)

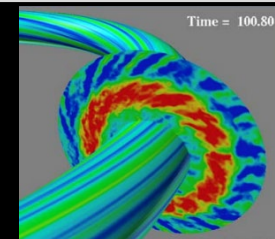


Ion-scale turbulence simulations in complex LHD plasma  
cf. Nunami, et al., Phys. Plasmas (2012)



Ion-scale turbulence simulations in simple Tokamak plasma

cf. Watanabe, et al., Nucl. Fusion (2006)





# Supercomputer Fugaku

158,976 nodes, 537 PFLOPS

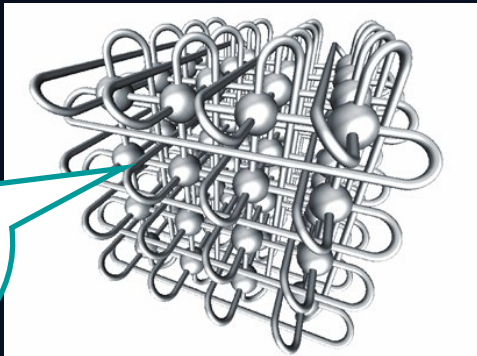
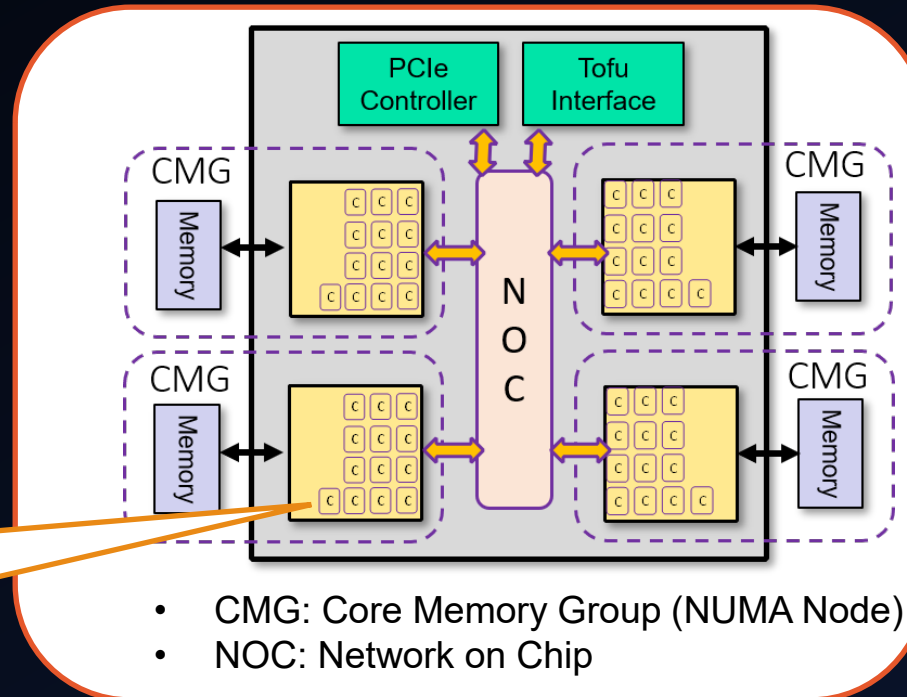


12 cores/CMG, 4 CMG/CPU

1 CPU/node

32 FLOP / (core · cycle)  
2.2 GHz

- 512-bit SIMD (SVE)
- 2FMA



6D Tofu interconnect  
(3D torus network  
from a user view)

# From K to Fugaku

	K	Fugaku
<b>System perf. [DP PFLOPS]</b>	10.6	537
<b># node/system</b>	82,944	158,976
<b># core/node</b>	8	48
<b>Node perf. [TFLOPS]</b>	0.128	3.38
<b>Core perf. [GFLOPS]</b>	16	70.4
<b>Memory size [GB]</b>	16	32
<b>Memory BW [GB/s]</b>	64	1024
<b>Memory Byte/FLOP</b>	<b>0.5</b>	<b>0.30</b>
<b>Interconnect BW [GB/s]</b>	20 (= 5.0 x 4)	40.8 (= 6.8 x 6)
<b>Interconnect Byte/FLOP</b>	<b>0.156</b>	<b>0.012</b>

Memory-BW-limited code can still be efficient.

Commun./Comput. cost ratio becomes much severe.  
→ Need to increase arithmetic intensity.

# Typical computation/communication of GKV

$$\frac{\partial \tilde{f}_s}{\partial t} + \left( v_{\parallel} \frac{\mathbf{B} + \tilde{\mathbf{B}}_{\perp}}{B} + \mathbf{v}_{sG} + \mathbf{v}_{sC} + \tilde{\mathbf{v}}_E \right) \cdot \nabla \tilde{f}_s + \frac{dv_{\parallel}}{dt} \frac{\partial \tilde{f}_s}{\partial v_{\parallel}} = S_s + C_s,$$

$$\nabla_{\perp}^2 \tilde{\phi} = -\frac{1}{\epsilon_0} \sum_s e_s (\tilde{n}_s + \tilde{n}_{s,pol}),$$

$$\nabla_{\perp}^2 \tilde{A}_{\parallel} = -\mu_0 \sum_s e_s \tilde{u}_{\parallel s},$$

- Domain decomposition of 5D phase space and plasma species  $\left( n_x, \frac{n_y}{P_w}, \frac{n_z}{P_z}, \frac{n_v}{P_v}, \frac{n_{\mu}}{P_{\mu}}, \frac{n_s}{P_s} \right)$
- Density/current evaluation: MPI\_allreduce among (v,m,s)
- Finite difference (z,v): MPI\_isend/irecv to (z,v)
- 2D FFT (x,y): MPI\_alltoall  $\left( n_x, n_y, \frac{n_v}{P_v}, \frac{n_z n_{\mu}}{P_z P_{\mu} P_w}, \frac{n_s}{P_s} \right) \rightarrow$  **Improved implementation** [Asahi'19CCPE]
- Implicit collision: MPI\_alltoall  $\left( n_v, n_{\mu}, n_s, \frac{n_z}{P_z}, \frac{n_x n_y}{P_w P_v P_{\mu} P_s} \right) \rightarrow$  **MPI-free iterative solver** [Maeyama'19CPC]

# Improved parallel spectral calculation

Spectral calculation of nonlinear advection  $N = v_x \partial_x f + v_y \partial_y f$  by transpose-split method.

- As-is (**y2x**):  $ik_x \hat{f}_k, ik_y \hat{f}_k \left( n_x, \frac{n_y}{P_w}, \frac{n_z}{P_z}, \frac{n_v}{P_v}, \frac{n_\mu}{P_\mu}, \frac{n_s}{P_s} \right) \rightarrow 1\text{D-FFT} \rightarrow \text{Transpose} \rightarrow 1\text{D-FFT} \rightarrow$   
 $\frac{\partial f}{\partial x}, \frac{\partial f}{\partial y} \left( \frac{n_x}{P_w}, n_y, \frac{n_z}{P_z}, \frac{n_v}{P_v}, \frac{n_\mu}{P_\mu}, \frac{n_s}{P_s} \right) \rightarrow \text{Nonlin. Adv.} \rightarrow \text{FFT} \rightarrow \text{Transpose} \rightarrow 1\text{D-FFT}$
- New (**y2zm**):  $\hat{f}_k \left( n_x, \frac{n_y}{P_w}, \frac{n_z}{P_z}, \frac{n_v}{P_v}, \frac{n_\mu}{P_\mu}, \frac{n_s}{P_s} \right) \rightarrow \text{Transpose} \rightarrow \hat{f}_k \left( n_x, n_y, \frac{n_v}{P_v}, \frac{n_z n_\mu}{P_z P_\mu P_w}, \frac{n_s}{P_s} \right) \rightarrow 2\text{D-FFT} \rightarrow$   
 Nonlin. Adv.  $\rightarrow 2\text{D-FFT} \rightarrow \text{Transpose}$

Pros: Data transpose is reduced. (**y2x**: 3 variables  $\rightarrow$  **y2zm**: 2 variables with 3/2 dealiasing)  
 $\rightarrow \sim \times 1.8$  speed up of nonlinear term (JFRS-1 192 node)

Cons: Wavenumber parallelization is limited up to  $\frac{n_z n_\mu}{P_z P_\mu} > P_w$ .

$\rightarrow$  Switch **y2zm** to **y2x** for a large number of parallelization  $P_w$ .

\* MPI\_alltoall among  $P_v P_\mu P_s$  in sub-communicators, not global commun.



# Implicit collision solver [Maeyama'19CPC]

When considering Coulomb collision, velocity-dependent collision frequency ( $\nu \propto 1/v^3$ ) severely restricts CFL.

## Our strategy

Since collision is an integro-differential operator over  $(v_{\parallel}, \mu, s)$ ,

1. Data transpose by MPI\_alltoall

$$f\left(n_x, \frac{n_y}{P_y}, \frac{n_z}{P_z}, \frac{n_v}{P_v}, \frac{n_{\mu}}{P_{\mu}}, \frac{n_s}{P_s}\right) = f\left(n_v, n_{\mu}, n_s, \frac{n_z}{P_z}, \frac{n_x n_y}{P_y P_v P_{\mu} P_s}\right)$$

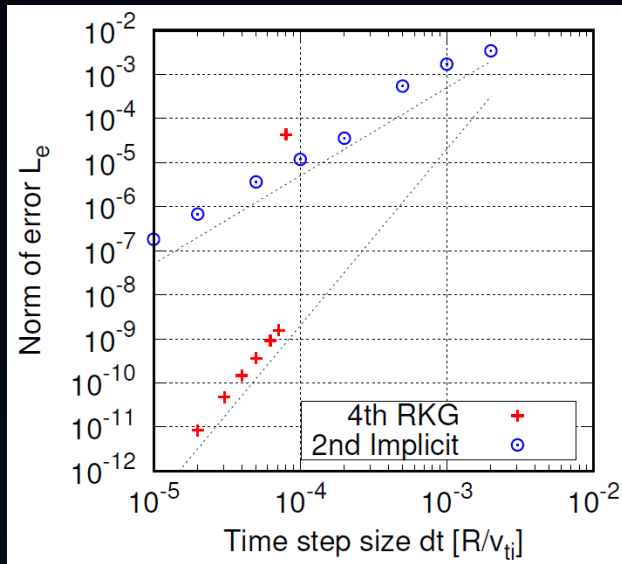
2. Iterative implicit solver for  $f(v_{\parallel}, \mu, s)$ , independent to  $(x, y, z)$ . (The iteration is MPI communication free!)
3. Transpose back again by MPI\_alltoall

\* MPI\_alltoall among  $P_v P_{\mu} P_s$  in sub-communicators, not global commun.

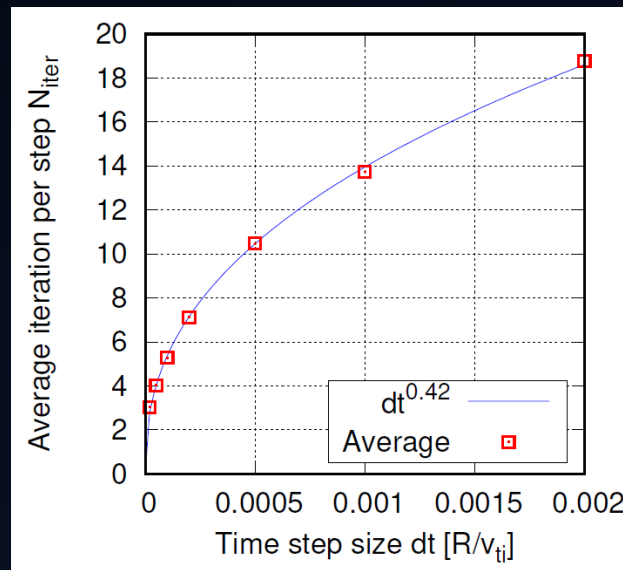
# Implicit collision solver [Maeyama'19CPC]

- ✓ Implicit solver allows stable computation over larger time steps.
- ✓ Arithmetic intensity and computational performance are enhanced.
  - Promising for manycore processor.

## Accuracy of the scheme



## Average iteration num.



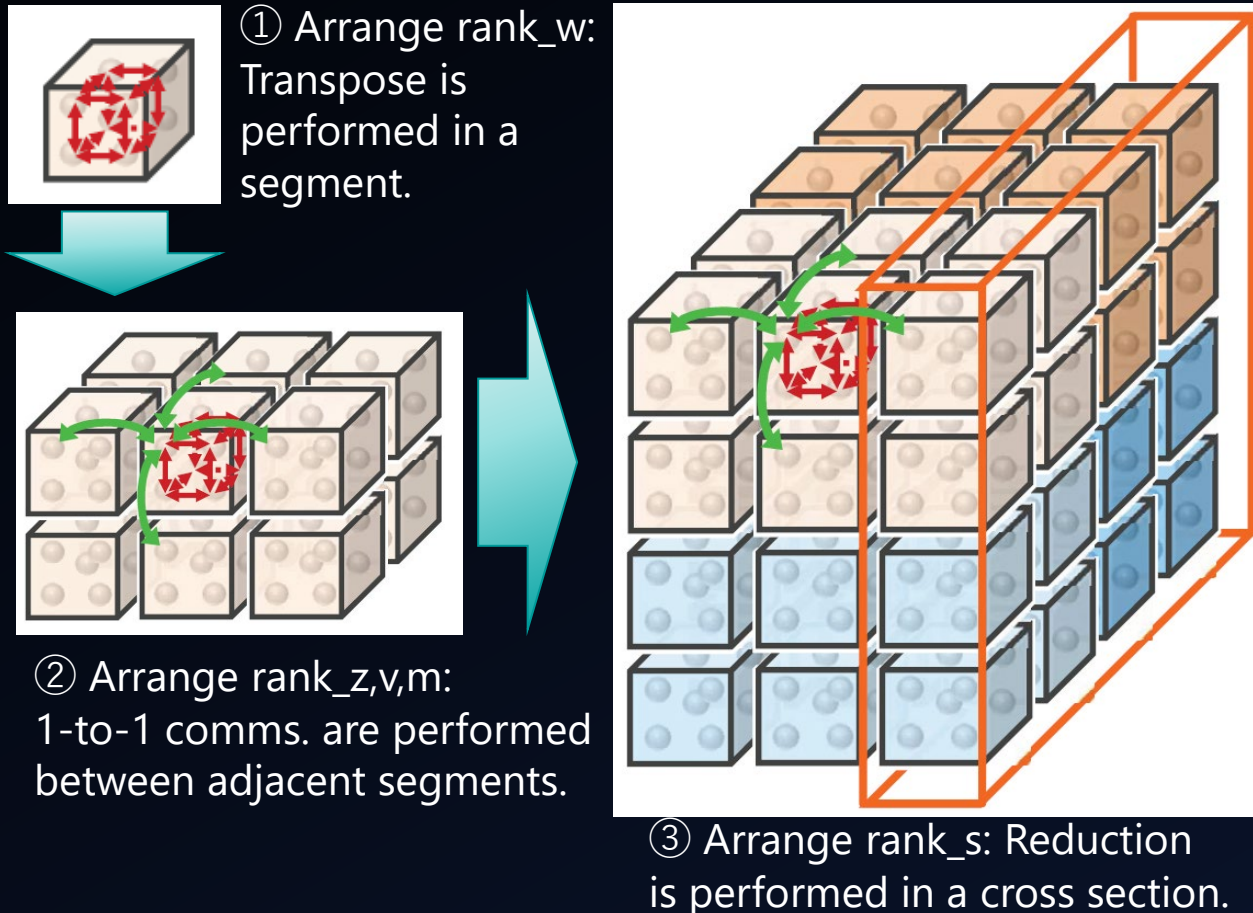
## Performance for a nonlinear run on FX100 ( $1.8 \times 10^{10}$ grids)

	4th Explicit	2nd Implicit
FLOPS (/PEAK)	8.67 TFLOPS (4.01%)	<b>25.78 TFLOPS (12.5%)</b>
Elapsed time per step	1.76 sec/step	3.13 sec/step
Time step size	$5 \times 10^{-5} R/v_{ti}$	$1 \times 10^{-3} R/v_{ti}$
Speed-up to solution	1	<b>10 times faster</b>

- Segmented MPI process mapping
- Pipelined computation-communication overlap

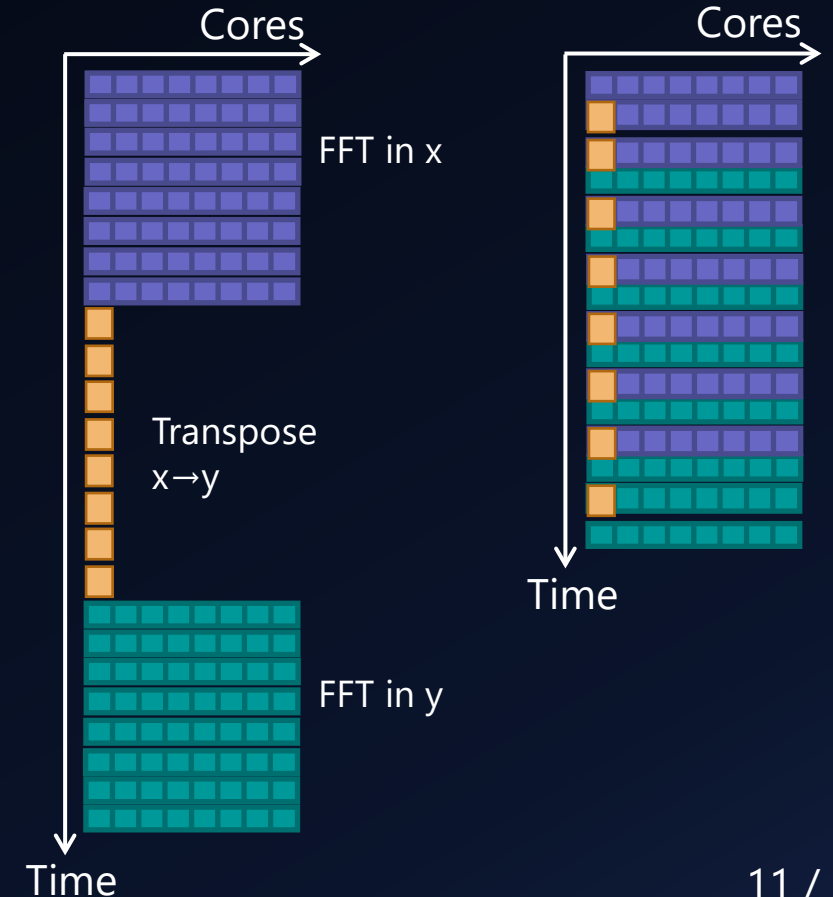
These techniques are available on Fugaku as well as K. [Maeyama'15PC]

### Process mapping on 3D torus network



### 2D-FFT w/o overlap

### 2D-FFT with overlap



# Weak scaling of GKV on Fugaku

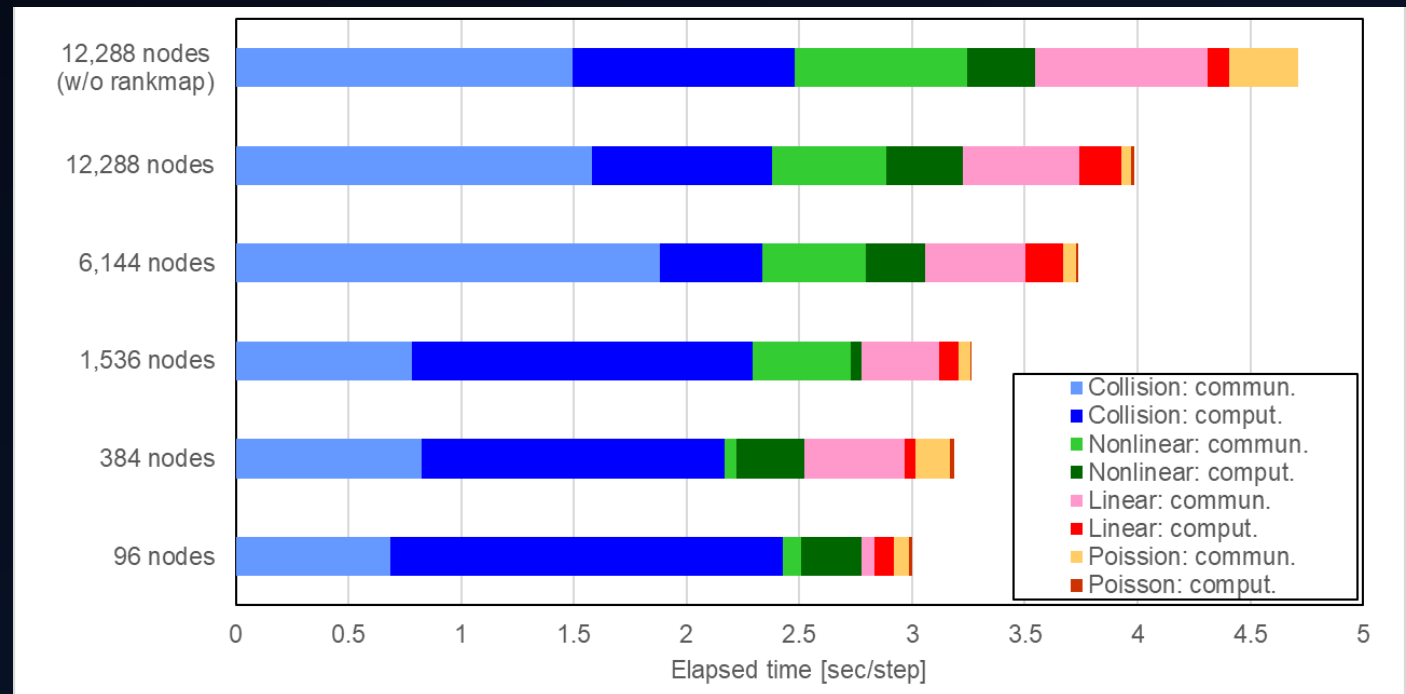
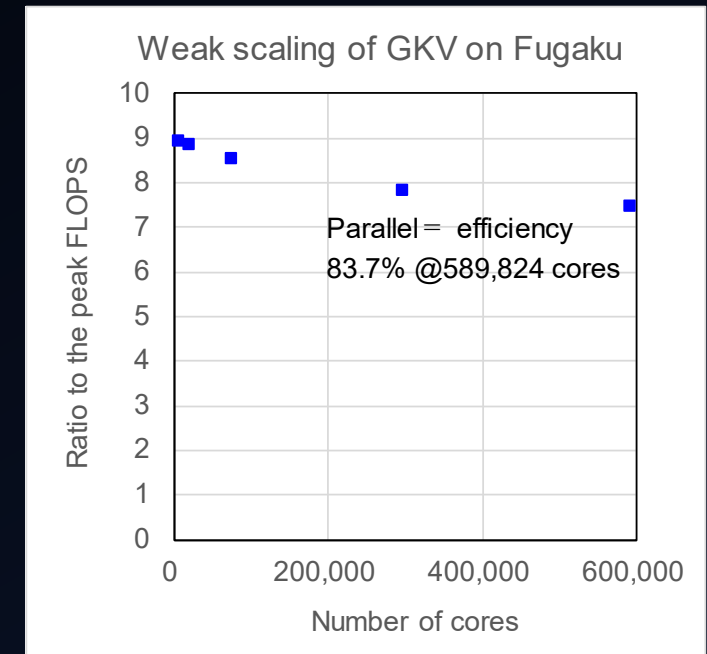
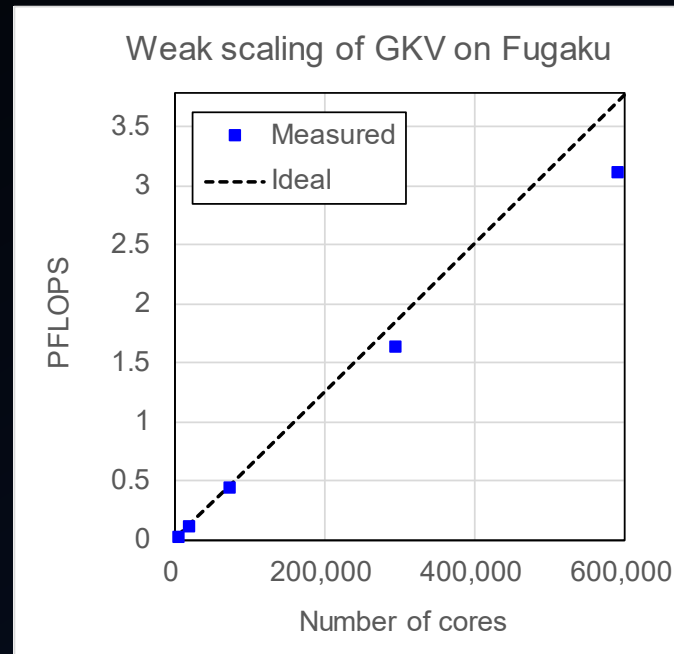
**Excellent scaling up to target problem size  $\sim 1.24 \times 10^{12}$  grids.**

(Fugaku 12,288 nodes, 589,824 cores, 49,152MPI, 12OpenMP, rankmap 8x32x48)

- ✓ 3.1PFLOPS
- ✓ 7.5% to peak FLOPS
- ✓ Parallel efficiency 83.7%

## Bottleneck of performance degradation

Communication costs of linear and nonlinear terms increase as grid and MPI number increases, which cannot be masked by related computations.



# Outline

- Optimization of GKV code on the supercomputer Fugaku - 10 min
- **Multi-scale turbulence simulations toward burning plasma - 10 min**



# Background

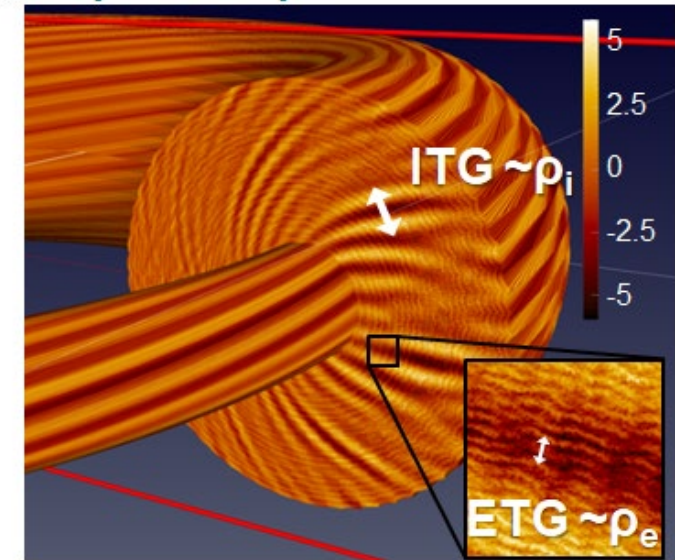
Recent gyrokinetic simulations reveal the importance of multi-scale interactions.

- Turbulent transport affected by electron scales [Maeyama'15PRL, Maeyama'17PRL]
- Multi-scale interactions are necessary to explain an experimental heat flux on Alcator C-Mod. [Howard'16NF]
- DIII-D results suggest the importance of multi-scale interactions in ITER [Holland'17NF]
- Recent multi-scale studies on JET [Bonanomi'18NF, Mantica'20PPCF, Mariani'21IAEA]

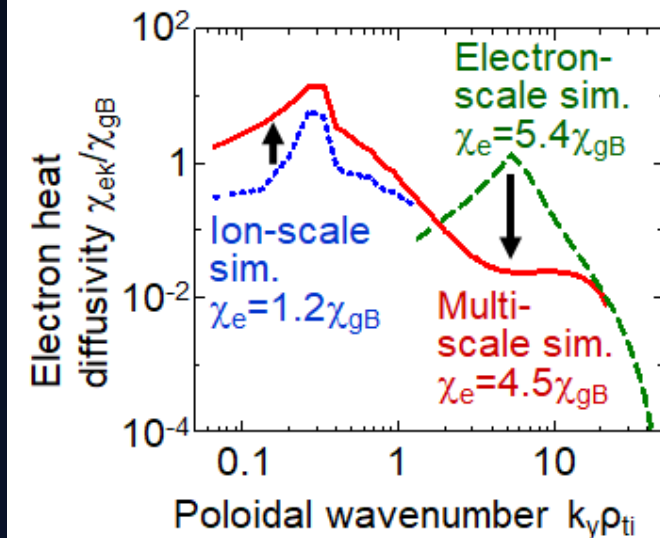
**Our physical target on Fugaku: Extrapolation of multi-scale interactions toward burning plasma**

- ✓ High electron temperature ( $T_e > T_i$ )
- ✓ Electron, Fuel (D,T), Ash (He) mixture

Snapshot of potential fluctuations



Turbulent transport spectrum

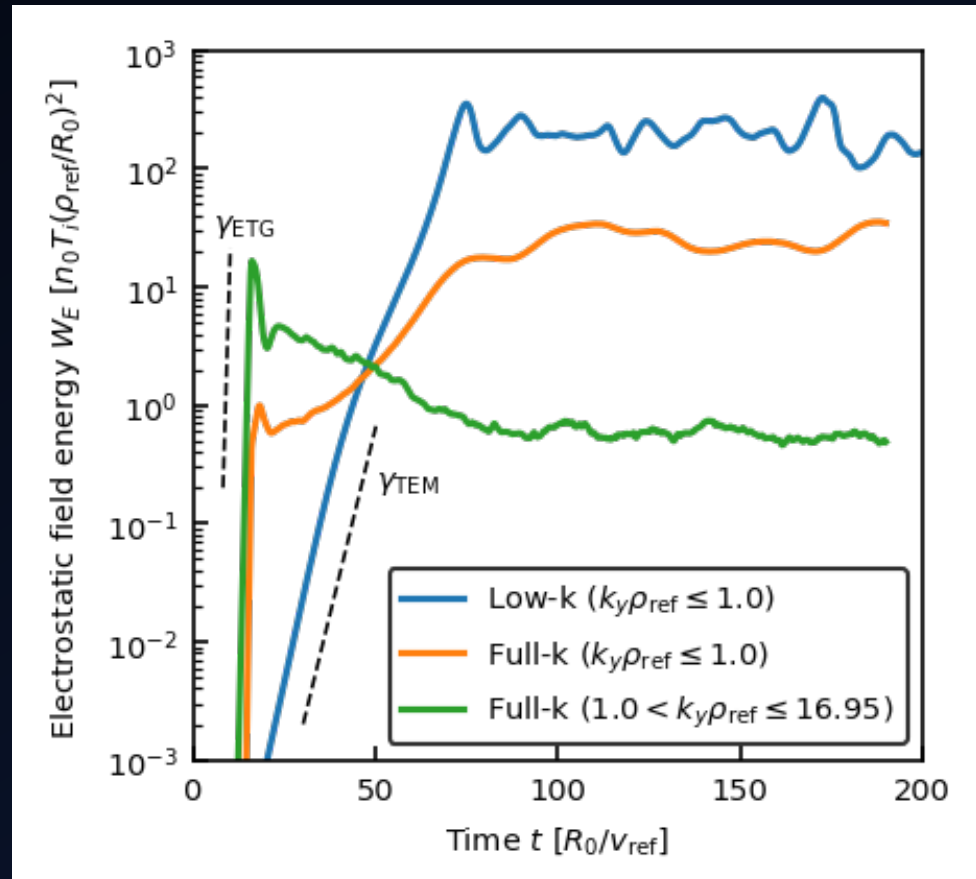


# TEM/ETG multi-scale turbulence simulation

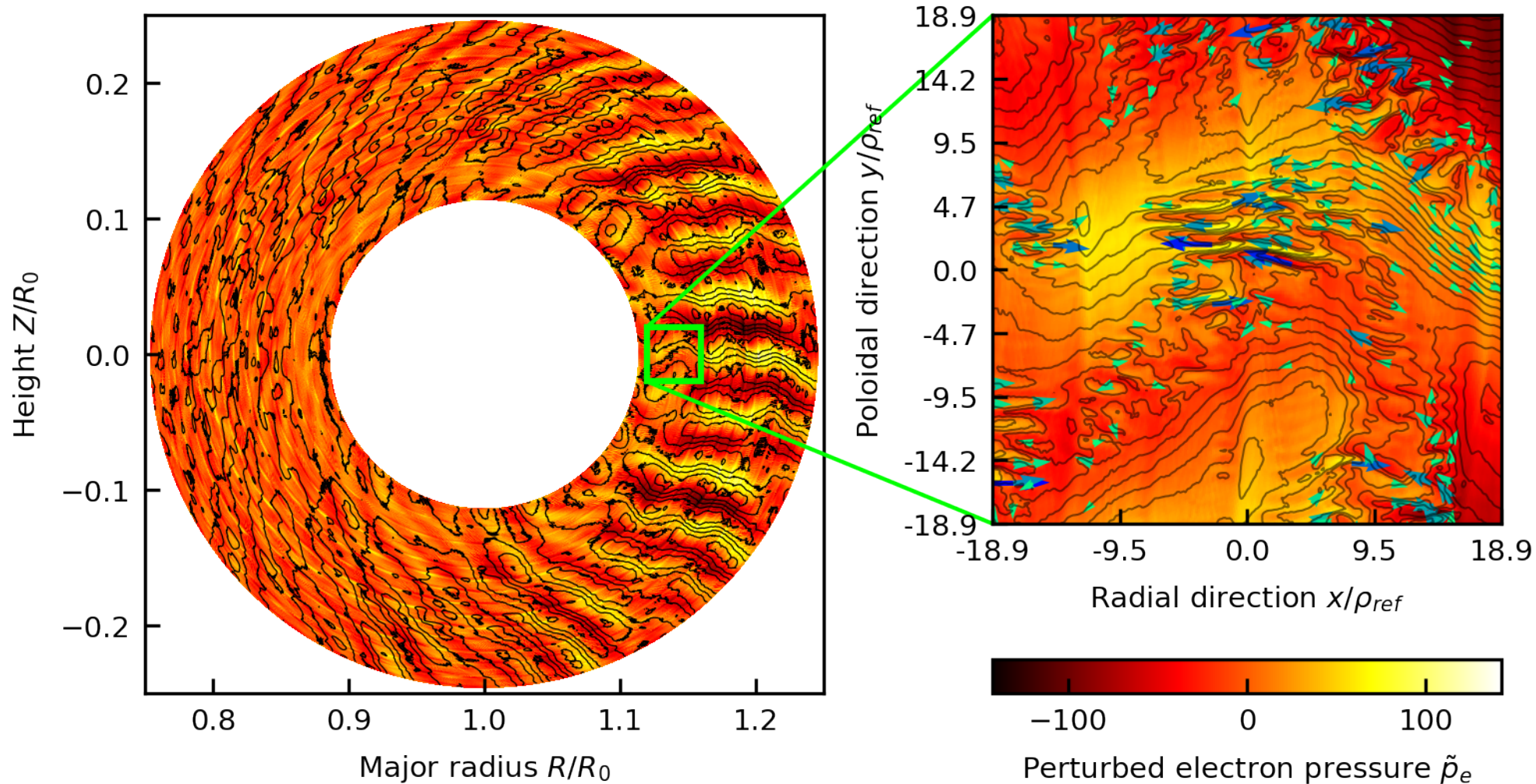
- ✓ **Electron temperature gradient modes (ETG)** grow initially. After that **trapped electron modes (TEM)** appear.
  - ◆ TEM growth rate is reduced in the presence of ETG turbulence.
  - ◆ TEM turbulence is suppressed in the presence of ETG turbulence.
- ETG stabilizes TEM.  
→ This suggests the importance of multi-scale interactions even in burning plasma.

## Time evolution of electrostatic energy

High-res. multi-scale simulation (Full-k) and low-res. ion-scale simulation (Low-k) are compared.



# Color map of perturbed electron pressure and streamlines of turbulent ExB flows



ETGs coexist with TEMs.

→ Small-scale ETG turbulence dissipatively stabilizes large-scale TEM.



# Impacts of turbulent transport

- ✓ **Large-to-small interactions: ETG peak is suppressed after TEM growth.**
- ✓ **Small-to-large interactions: TEM amplitude is also reduced in the presence of ETG.**

Comparison of heat flux [gyro-Bohm unit]

Electron :  $Q_e = 524$  (low-k)  $\rightarrow$  88 (Full-k)

Fuel :  $Q_D + Q_T = 17$  (Low-k)  $\rightarrow$  3.7 (Full-k)

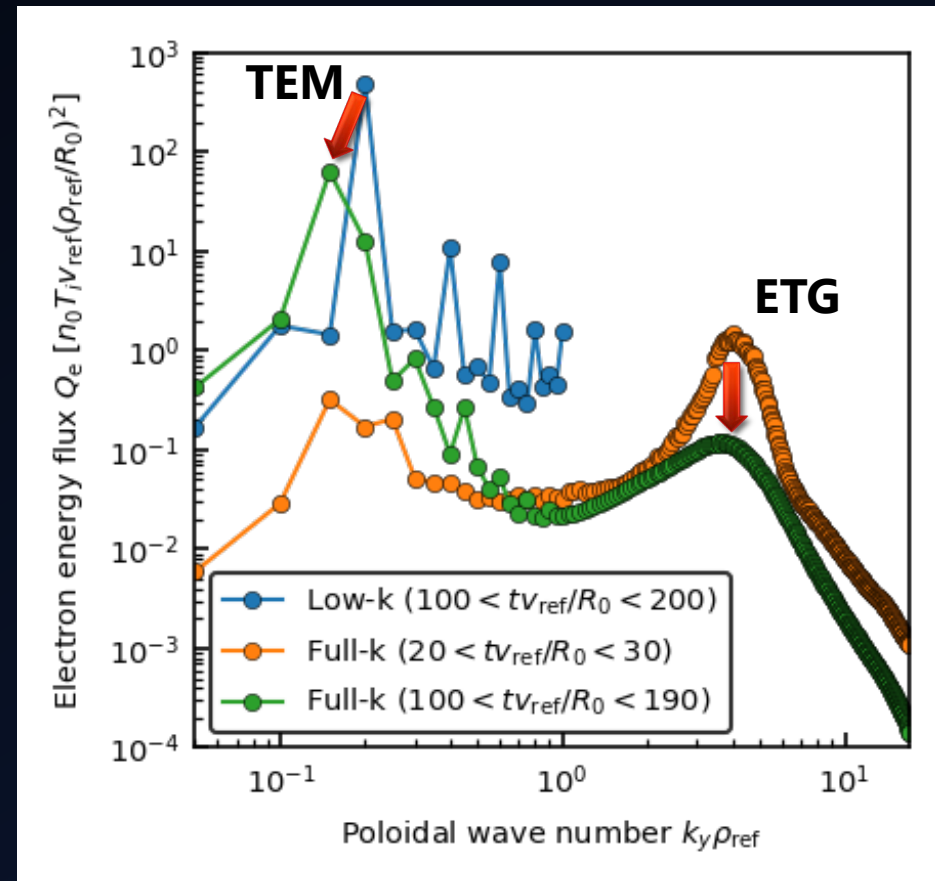
Ash :  $Q_{He} = 1.4$  (low-k)  $\rightarrow$  0.3 (Full-k)

**$\rightarrow$  This result firstly demonstrates the possibility of reduction of  $Q_e$  by cross-scale interactions.**

$\rightarrow$  It affects not only electrons but also fuel ions and helium ash.

## Wavenumber spectra of electron energy flux

High-res. multi-scale simulation (Full-k) and low-res. ion-scale simulation (Low-k) are compared.



# Velocity-space structures

- ✓ Velocity-space dependent turbulent flux

$$\Gamma_e^v(z, v_{\parallel}, \mu) = \int_0^{L_x} \frac{dx}{L_x} \int_0^{L_y} \frac{dy}{L_y} \left( \frac{-\nabla J_0 \tilde{\phi} \times \mathbf{b}}{B_0} \cdot \nabla x \right) \tilde{f}_e$$

Cf.

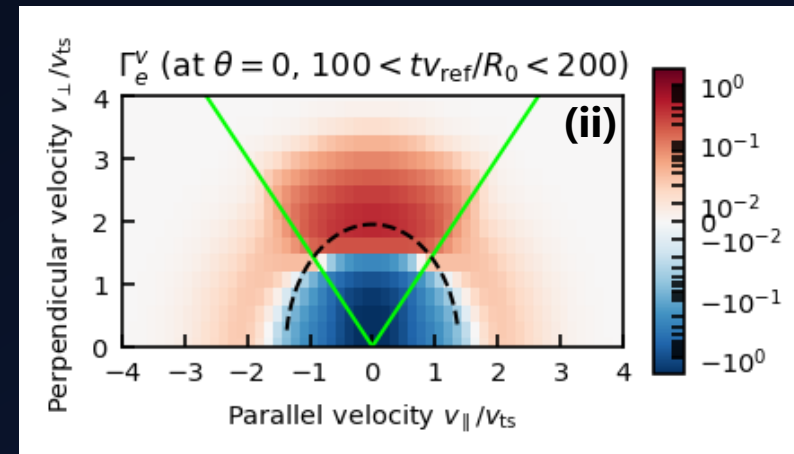
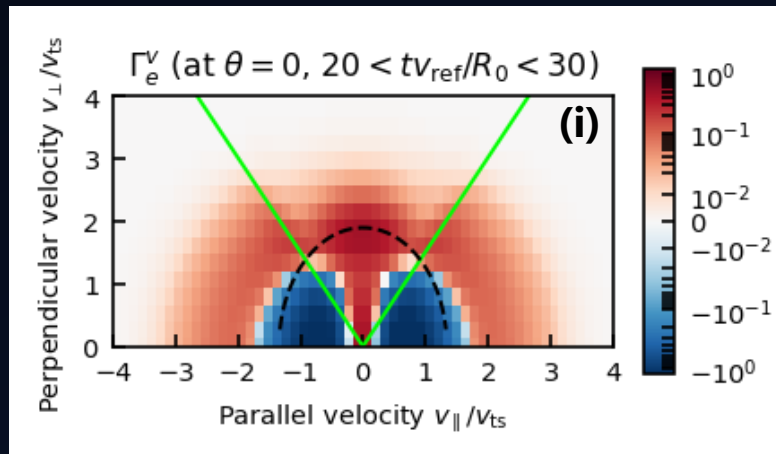
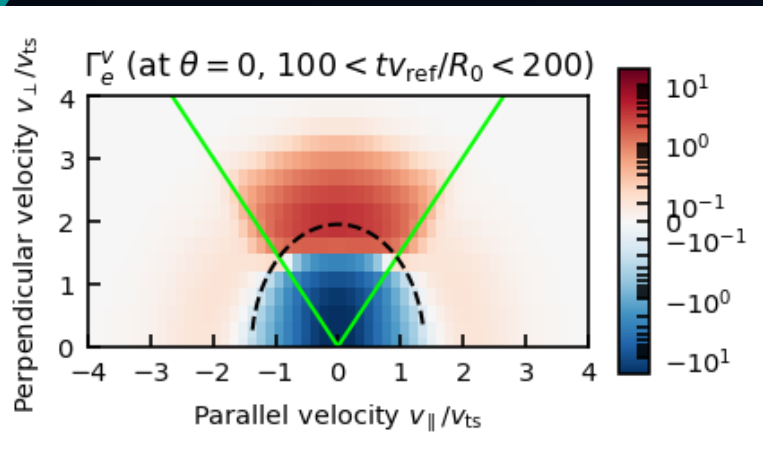
$$\text{Particle flux } \Gamma_e = \left\langle \int_{-\infty}^{\infty} dv_{\parallel} \int_0^{\infty} dv_{\perp} 2\pi v_{\perp} \Gamma_e^v(z, v_{\parallel}, \mu) \right\rangle$$

$$\text{Energy flux } Q_e = \left\langle \int_{-\infty}^{\infty} dv_{\parallel} \int_0^{\infty} dv_{\perp} 2\pi v_{\perp} \frac{m_e v^2}{2} \Gamma_e^v(z, v_{\parallel}, \mu) \right\rangle$$

- ✓ Isotropic dependence by magnetic drift resonance of toroidal ETG. [black dotted line]
- ✓ Precession drift resonance by trapped electron [between green lines] dominates in TEM.

Low-res. ion-scale sim. (Low-k)

High-res. multi-scale sim. (Full-k) (i) initial ETG, (ii) TEM/ETG saturated.





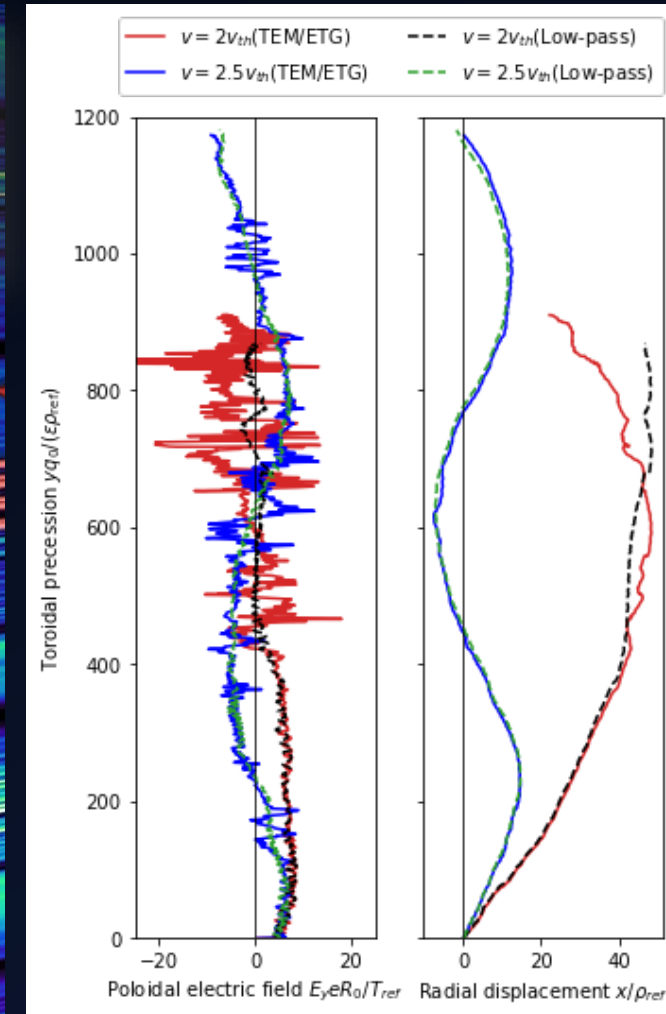
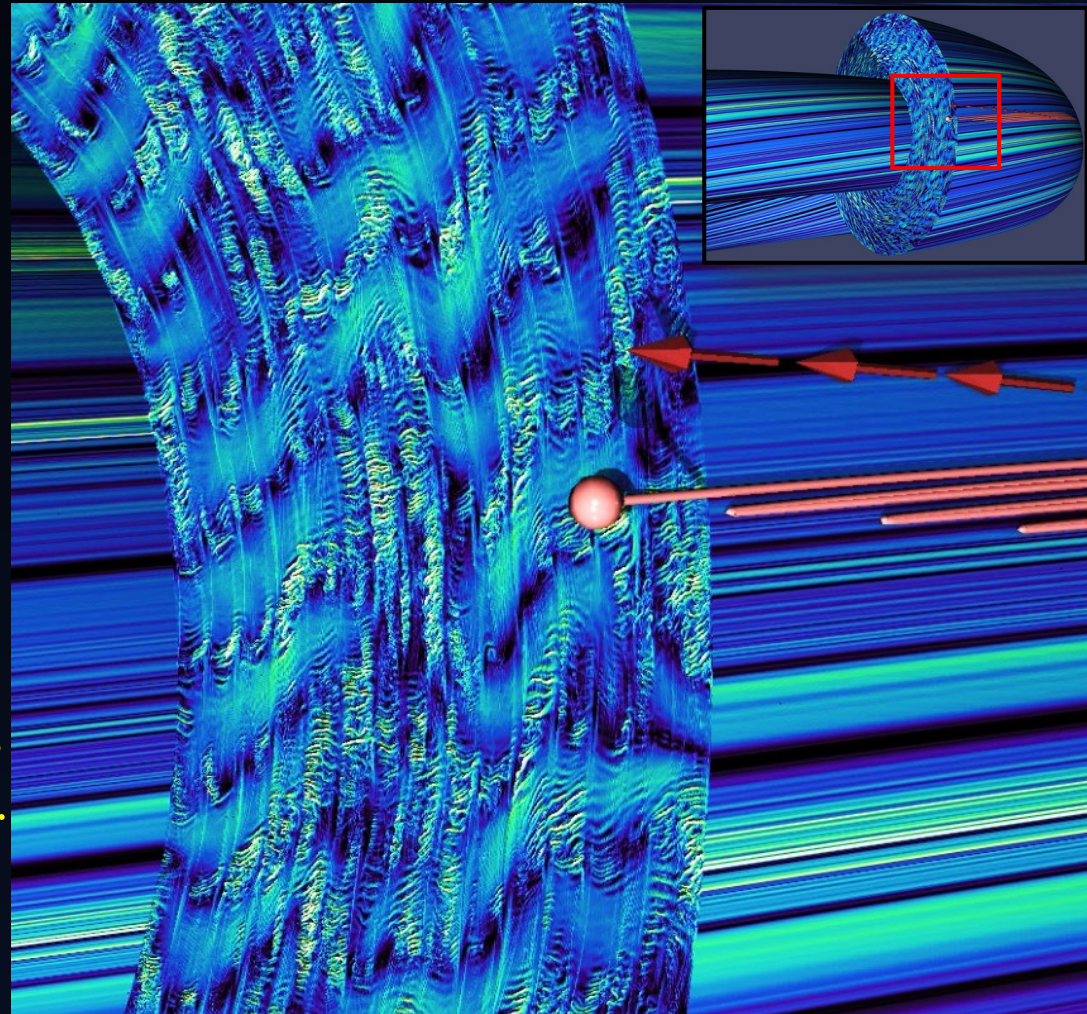
# Schematic explanation of TEM/ETG cross-scale interactions

Small-to-large interactions:

- ✓ ETG turbulence distorts trapped electron trajectory, and reduces the precession drift resonance of TEM.

Large-to-small interactions:

- ✓ TEM turbulent eddies shears ETG streamers. (even when no strong zonal flows [Asahi'14PoP] )



# Summary

## HPC

- ✓ Physical applicability of GKV is extended along with HPC.
- ✓ High Memory-Byte/FLOP=0.30 but low Interconnect Byte/FLOP=0.012 on Fugaku.
  - Reduce communication cost of GKV by mapping, overlap, improved implementation.
- ✓ GKV achieves excellent scaling and 3.1 PFLOPS (7.5% to peak) on Fugaku 12,288 nodes

## Physics

- ✓ Multi-scale turbulence simulation toward burning plasma (High  $T_e > T_i$ , mixture of e,D,T,He)
- ✓ Cross-scale interactions changes turbulent spectrum, which affect turbulent transport levels of not only electron but also fuel D,T and He ash.
- ✓ **The result firstly demonstrated the possibility of reduction of  $Q_e$  by cross-scale interactions.**
- ✓ Large-to-small interactions: TEM turbulent eddies suppress ETG streamers
- ✓ Small-to-large interactions: ETG stabilizes TEM by disturbing precession drift resonance
  - Analogy 1: damping of short-wave-length zonal flow by ETG [Maeyama'15PRL; Maeyama'17NF]
  - Analogy 2: destruction of MTM current sheet by ETG [Maeyama'17PRL]
- ✓ Mutual exclusive nature between disparate-scale turbulence